

Design of a Single-Phase PV Fed Nine Level Inverter to Drive an Induction Motor

K.Sharmila Sowjanya¹, Sri. M. Gopichand Naik², J.V.G. Rama Rao³

¹Department of Electrical Engineering
Andhra University, Visakhapatnam, India
sharmilasowjanya@gmail.com

²Department of Electrical Engineering
Andhra University, Visakhapatnam, India
gopi_525@yahoo.co.in

³Department of Electrical Engineering
B.V.C. Engineering College, Odalarevu, India

Abstract: Single Phase induction motors are widely accepted motor due to their energy efficient characteristics. To drive varying mechanical loads for long duty, the machine needs to be controlled to increase its efficiency and minimize harmonics. This paper presents the voltage control method using semiconductor power devices for a single-phase induction motor in order to achieve a smooth, continuous and low total harmonics distortion (THD) waveforms. This paper implements a new single-phase nine-level inverter fed with photovoltaic systems, with a pulse width-modulated (PWM) control scheme which is used to generate the PWM signals for the inverter. This multilevel inverter allows Maximum Power Point Tracking (MPPT) to extract maximum power from the sun when it is available. An adaptive MPPT algorithm is used with a standard perturb and observe method for the PV system. A boost converter is used to step up the input voltage of the inverter interposed between the PV array and Nine-Level Inverter. This new nine-level inverter with reduced number of switches converts DC to AC which is capable of producing nine levels of output-voltage levels (V_{dc} , $3V_{dc}/4$, $V_{dc}/2$, $V_{dc}/4$, 0 , $-V_{dc}/4$, $-V_{dc}/2$, $-3V_{dc}/4$, $-V_{dc}$) from the dc supply voltage. The Pulse Width Modulation (PWM) signals are generated to the inverter by using PID and Fuzzy Controllers and the total harmonic distortion (THD) results are compared. The LC-filter is modeled to obtain pure sine-wave and is given to drive a single-phase induction motor. The voltage control of Single-Phase Induction Motor for better performance is modeled and implemented in MATLAB / SIMULINK environment. The Simulation circuit is analyzed and results are presented for the system.

Keywords: multilevel inverter, photovoltaic (PV) system, pulse width-modulated (PWM), total harmonic distortion (THD). MPPT

1. Introduction

The ever-increasing energy consumption, fossil fuels soaring costs and exhaustible nature, and worsening global environment have created a booming interest in renewable energy generation systems, one of which is photovoltaic. Such a system generates electricity by converting the Sun's energy directly into electricity. Photovoltaic-generated energy can be delivered to drive electrical machines (Induction Motor) through inverters.

When the motor is started, it draws high starting current. This high current cause's dip in the voltage and distorts the voltage waveform; therefore it is necessary to take into account the remedial measures to remove harmonics in the single phase induction motor.

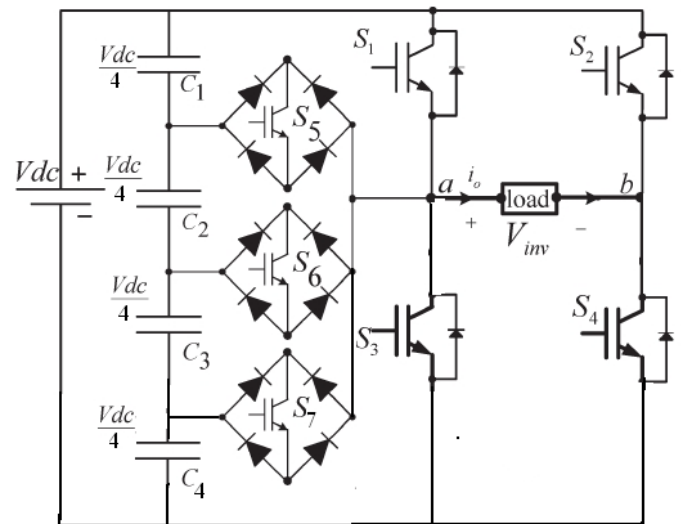


Figure 1: Single-Phase Nine-Level Inverter for a Motor load

Hence a multilevel Inverter is needed to reduce the harmonics in the voltage waveform of the Single-Phase Induction Motor which results in better Total Harmonic Distortion (THD) Content and improves the performance of the motor.

A single-phase inverter is usually used for residential or low-power applications of power ranges that are less than a kW. One of the significant advantages of multilevel

inverters configuration is the harmonic reduction in the output waveform without increasing switching frequency or decreasing the inverter power output. The output voltage waveform of a multilevel inverter is composed of the number of voltages, typically obtained from capacitor voltage sources. Multilevel starts from three levels. As number of levels reach infinity, the output THD approaches zero. The number of the achievable voltage levels, however, is limited by voltage unbalance problems, voltage clamping requirement, circuit layout and packaging constraints.

2. Multilevel Inverter Topology

The single-phase nine-level inverter was developed from the seven-level inverter as shown in Fig.1. It comprises a single-phase conventional H-bridge inverter, three bidirectional switches, and a capacitor voltage divider formed by C1, C2, C3 and C4, as shown in Fig. 1. The modified H-bridge topology is significantly advantageous over other topologies, i.e., less power switch, power diodes, and less capacitor for inverters of the same number of levels. Photovoltaic (PV) arrays were connected to the inverter via a dc-dc boost converter. The power generated by the inverter is to be delivered to induction Motor.

The dc-dc boost converter was required because the PV arrays had a voltage that was lower than the single-phase voltage. High dc bus voltages are necessary to ensure that power flows from the PV arrays to the single-phase induction motor. The LC-filter is modeled to obtain pure sine-wave and is given to drive a single-phase induction motor. Proper switching of the inverter can produce nine-output-voltage-levels (V_{dc} , $3V_{dc}/4$, $V_{dc}/2$, $V_{dc}/4$, 0, $-V_{dc}/4$, $-V_{dc}/2$, $-3V_{dc}/4$, $-V_{dc}$) from the dc supply voltage.

The proposed inverter's operation can be divided into nine switching states. The required nine levels of output voltage were generated as follows.

Maximum positive output (V_{dc}): S1 is ON, connecting the load positive terminal to V_{dc} , and S4 is ON, connecting the load negative terminal to ground. All other controlled switches are OFF; the voltage applied to the load terminals is V_{dc} .

Three-fourth positive output ($3V_{dc}/4$): The bidirectional switch S5 is ON, connecting the load positive terminal, and S4 is ON, connecting the load negative terminal to ground. All other controlled switches are OFF; the voltage applied to the load terminals is $3V_{dc}/4$.

Half of the positive output ($V_{dc}/2$): The bidirectional switch S6 is ON, connecting the load positive terminal, and S4 is ON, connecting the load negative terminal to ground. All other controlled switches are OFF; the voltage applied to the load terminals is $V_{dc}/2$.

One-fourth of the positive output ($V_{dc}/4$): The

bidirectional switch S7 is ON, connecting the load positive terminal, and S4 is ON, connecting the load negative terminal to ground. All other controlled switches are OFF; the voltage applied to the load terminals is $V_{dc}/4$.

Zero output: This level can be produced by two switching combinations; switches S3 and S4 are ON, or S1 and S2 are ON, and all other controlled switches are OFF; terminal ab is a short circuit, and the voltage applied to the load terminals is zero.

One-fourth negative output ($-V_{dc}/4$): The bidirectional switch S5 is ON, connecting the load positive terminal, and S2 is ON, connecting the load negative terminal to V_{dc} . All other controlled switches are OFF; the voltage applied to the load terminals is $-V_{dc}/4$.

Half of the negative output ($-V_{dc}/2$): The bidirectional switch S6 is ON, connecting the load positive terminal, and S2 is ON, connecting the load negative terminal to ground. All other controlled switches are OFF; the voltage applied to the load terminals is $-V_{dc}/2$.

Three-fourth negative output ($-3V_{dc}/4$): The bidirectional switch S7 is ON, connecting the load positive terminal, and S2 is ON, connecting the load negative terminal to ground. All other controlled switches are OFF; the voltage applied to the load terminals is $-3V_{dc}/4$.

Maximum negative output ($-V_{dc}$): S2 is ON, connecting the load negative terminal to V_{dc} , and S3 is ON, connecting the load positive terminal to ground. All other controlled switches are OFF; the voltage applied to the load terminals is $-V_{dc}$.

Table I shows the switching combinations that generated the nine output-voltage levels (V_{dc} , $3V_{dc}/4$, $V_{dc}/2$, $V_{dc}/4$, 0, $-V_{dc}/4$, $-V_{dc}/2$, $-3V_{dc}/4$, $-V_{dc}$)

Table 1: Output Voltage According to the Switches' On Off Condition

V_o	S_1	S_2	S_3	S_4	S_5	S_6	S_7
V_{dc}	On	Off	Off	On	Off	Off	Off
$3V_{dc}/4$	Off	Off	Off	On	On	Off	Off
$V_{dc}/2$	Off	Off	Off	On	Off	On	Off
$V_{dc}/4$	Off	Off	Off	On	Off	Off	On
0	On	On	Off	Off	Off	Off	Off
$V_{dc}/4$	Off	On	Off	Off	On	Off	Off
$-V_{dc}/2$	Off	On	Off	Off	Off	On	Off
$-3V_{dc}/4$	Off	On	Off	Off	Off	Off	On
$-V_{dc}$	Off	On	On	Off	Off	Off	Off

3. Block Diagrams

The block diagrams of the single-phase Pv fed nine-level inverter to drive an induction motor are shown in Figures.

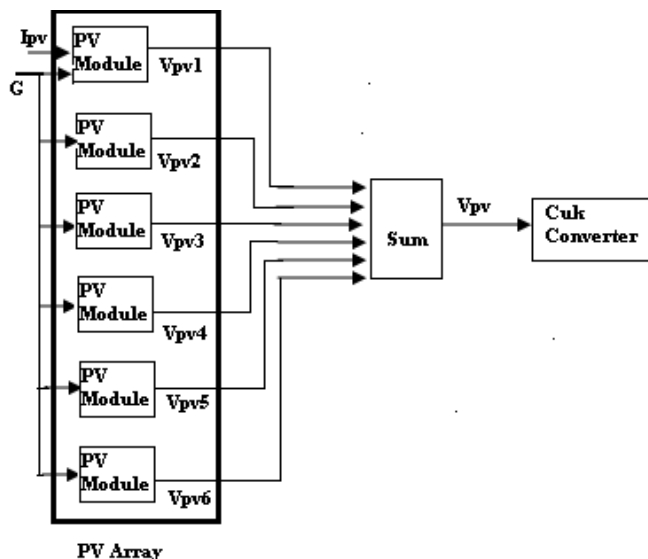


Figure 2: Block diagram of PV Array

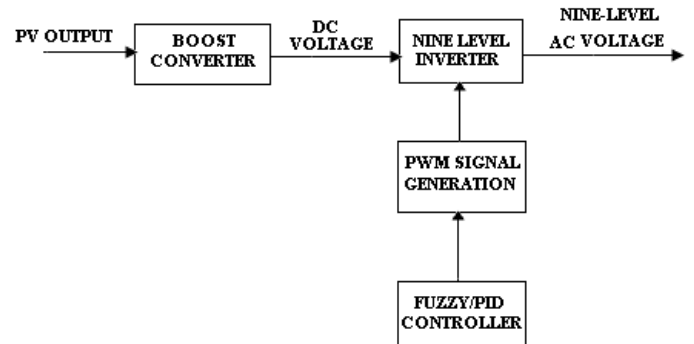


Figure 3: Block Diagram of Nine-Level Inverter

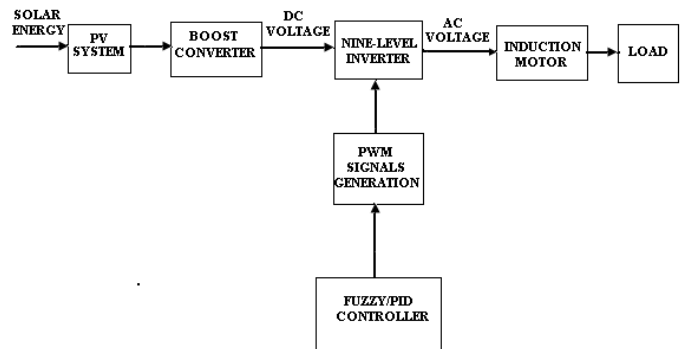


Figure 4: Block Diagram of the Overall System

4. MPPT Control of the System

A common inherent drawback of PV and system is the intermittent nature of their energy source. Solar energy is present throughout the day, but the solar irradiation levels vary due to sun intensity and unpredictable shadows cast by clouds, birds, trees, etc. These drawbacks tend to make these renewable systems inefficient. However, by incorporating maximum power point tracking (MPPT) algorithms, the systems' power transfer efficiency can be improved significantly.

A solar cell is comprised of a P-N junction semiconductor that produces currents via the photovoltaic effect.

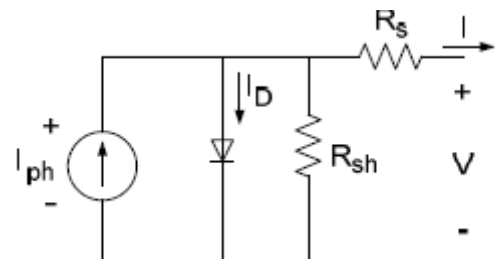


Figure 5: PV cell equivalent circuit

PV arrays are constructed by placing numerous solar cells connected in series and in parallel. A PV cell is a diode of a large-area forward bias with a photo voltage and the equivalent circuit is shown by Figure 10. The current-voltage characteristic of a solar cell is derived in as follows:

$$I = I_{ph} - I_D \tag{14}$$

$$I = I_{ph} - I_0 \exp\left[\frac{q(V+R_S I)}{AK_B T} - 1\right] - \frac{V+R_S I}{R_{Sh}} \tag{15}$$

Where

- I_{ph} = photocurrent,
- I_D = diode current,
- I₀ = saturation current,
- A = ideality factor,
- q = electronic charge 1.6x10⁻¹⁹,
- k_B = Boltzmann's gas constant (1.38x10⁻²³),
- T = cell temperature,
- R_s = series resistance,
- R_{sh} = shunt resistance,

I = cell current,
V = cell voltage.

Typically, the shunt resistance (R_{sh}) is very large and the series resistance (R_s) is very small. Therefore, it is common to neglect these resistances in order to simplify the solar cell model. The resultant ideal voltage-current characteristic of a photovoltaic cell is given by (16) and illustrated by Figure 11.

$$I = I_{ph} - I_0 \left[\exp\left(\frac{qV}{KT}\right) - 1 \right] \tag{16}$$

Therefore by adjusting the output current (or voltage) of the PV array, maximum power from the array can be drawn. Due to the similarities of the shape of the wind and PV array power curves, a similar maximum power point tracking scheme known the standard perturb and observe method is often applied to these energy sources to extract maximum power.

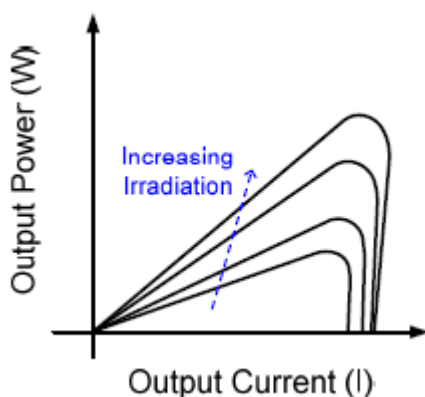


Figure 6: PV cell power characteristics

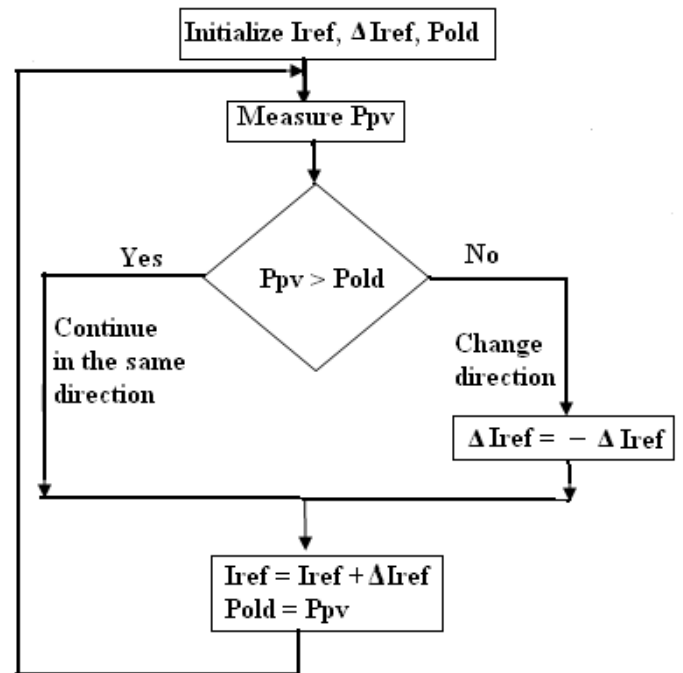


Figure 7: General MPPT Flow Chart for PV

The standard perturbs and observes method for the PV system. This perturbs the operating point of the system and observes the output. If the direction of the perturbation (e.g an increase or decrease in the output voltage of a PV array) results in a positive change in the output power, then the control algorithm will continue in the direction of the previous perturbation. Conversely, if a negative change in the output power is observed, then the control algorithm will reverse the direction of the previous perturbation step. In the case that the change in power is close to zero (within a specified range) then the algorithm will invoke no changes to the system operating point since it corresponds to the maximum power point (the peak of the power curves). Figure 13 is the flow chart that illustrates the implemented MPPT scheme.

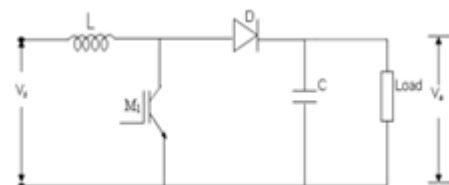


Figure 8: Circuit diagram of Boost Converter

5. DC-DC Boost Converter Model

The dc–dc boost converter was required because the PV arrays had a voltage that was lower than the single-phase voltage to drive the Induction Motor. Hence it is modeled. Boost converter is a power electronic circuit which gives the output voltage which is greater than the input voltage. It consists of dc input voltage source V_s , boost inductor L , controlled switch S , diode D , filter capacitor C , and load resistance R . The circuit diagram of boost converter is shown in Fig.8

Using Faraday’s law for the boost inductor

$$V_s DT = (V_o - V_s) / (1 - D) T$$

From which the dc voltage transfer function turns out to be

$$M_v = \frac{V_o}{V_s} = \frac{1}{1 - D}$$

As the name of the converter suggests, the output voltage is always greater than the input voltage. The boost converter operates in the CCM for $L > L_b$ where

$$L_b = \frac{(1 - D)^2 DR}{2f}$$

Where d, is the duty ratio of dc to dc converter which is defined as the ratio of turn on time to that of total time. The boost converter steps up the voltage from PV array to the required value before feeding to the Nine-Level Inverter system.

6. Single-Pulse-Width-Modulation (SPWM)

In single pulse width modulation control there is only one pulse per half cycle and the output rms voltage is changed by varying the width of the pulse. The gating signals to the inverter are generated by comparing the rectangular control signal of amplitude V_c with triangular carrier signal V_{car} .

7. Design of LC Filter

Filters play a key role in the inverter driven loads. It is mainly used for two reasons. They are as listed below.

1. To convert the inverter output (i.e., square wave) into pure sinusoidal wave
2. To eliminate the higher order harmonics.

7.1 LC-Filter

In this project, we use LC-filter. LC-filter is a second order filter and it has better filtering ability than L-filter. This simple configuration is easy to design and it works mostly without problems. The basic block diagram of a LC-filter is as shown below in Fig.9

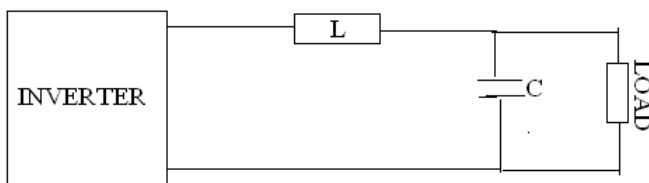


Figure 9: Block Diagram of LC Filter

7.2 Modeling of LC-Filter

In filter designing, the first step is finding the best filter.

The second step is calculating the designed impedance from the lowest voltage (V_{min}) divided by the highest current (I_{max}) where is R_d . The third step is equating the inductor (L) and the capacitor (C) values from the second step using the following equation.

The design impedance form can be calculated by using the below equation

$$R_d = \frac{V_{min}}{I_{max}}$$

The inductance (L) and the capacitance (C) values of the filter can be calculated by

$$L = \frac{R_d}{2\pi f}$$

$$C = \frac{1}{2\pi f R_d}$$

8. 8. MATLAB / SIMULINK Model for Overall System

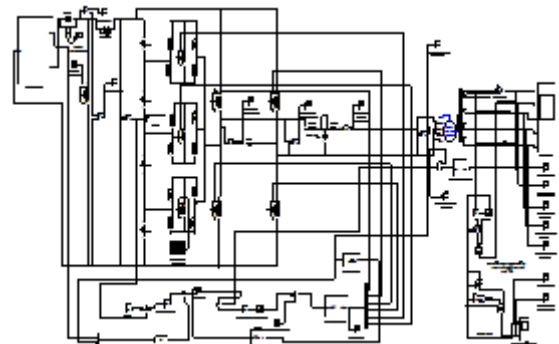


Figure 10: SIMULINK model for Overall solar, Nine-level Inverter with Induction Motor system

9. Results and Discussions

The simulated results of the proposed nine-level inverter without and with filter, induction motor are presented below

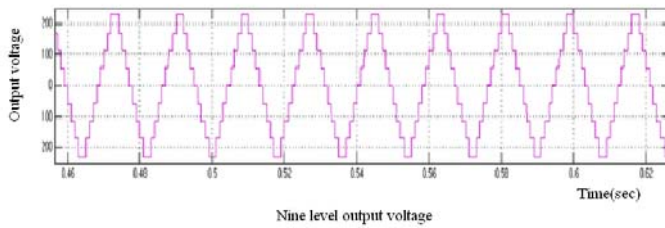


Figure 11: Nine-Level Inverter Voltage

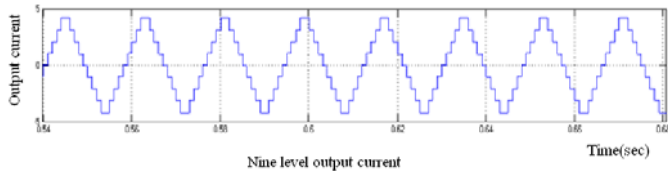


Figure 12: Nine-Level Inverter Current

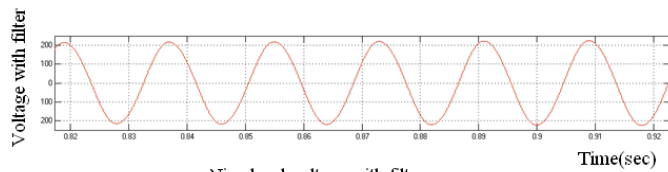


Figure 13: Nine-Level Inverter Voltage with Filter

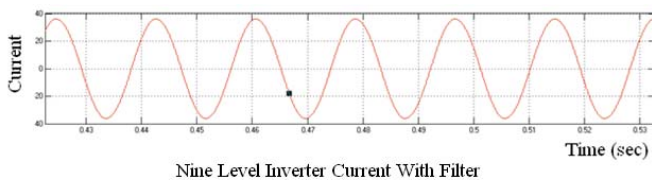


Figure 14: Nine-Level Inverter Current With Filter

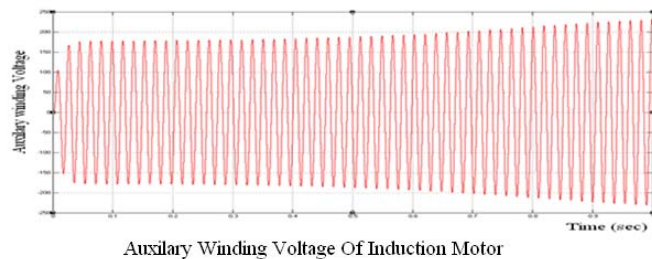


Figure 15: Auxiliary Winding Voltage Of Induction Motor

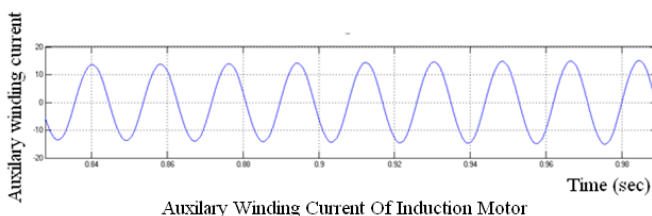


Figure 16: Auxiliary Winding Current Of Induction Motor

9.1 THD Results

Table 2: Comparison of THD levels of Nine-Level Inverter with and without filter by using PID and Fuzzy controllers

Controller	Nine-Level Inverter Output THD Without Filter		Nine-Level Inverter Output THD With Filter	
	Voltage	Current	Voltage	Current
PID	14.53	14.53	4.87	6.24
Fuzzy	14.51	14.51	4.35	5.38

It is observed that the THD result of Nine-Level Inverter with Fuzzy controller is better when compared to PID controller to drive an Induction Motor for better performance of its utilization.

10. Conclusion

Multilevel inverters offer improved output waveforms at lower THD. This paper has presented a SPWM technique is used to control the IGBT Nine-Level inverter which utilizes reference signal and a triangular carrier signal to generate PWM switching signals. The behavior of the proposed multilevel inverter was analyzed in detail. The THD results of Nine-level inverter are compared with PID and Fuzzy controllers is an attractive solution for the PV connected inverters. The PV system employs Maximum power point tracking (MPPT) feature is realized by standard perturbation and observation method.

The boost converter is designed and implemented which is used to step up the low input voltage produced by PV array. This system is successfully modeled to drive a single-phase induction motor for smooth starting by effectively eliminating of lower order harmonics, where higher order harmonics are eliminated by using LC filter for better efficiency of its utilization which improves the motor performance. The integrated system is easy to implement and economical.

References

- [1] B.R.Sanjeeva Reddy, Praveen Jambholkar, P.Badari Narayana, Prof. K. Srinivasa Reddy “ MPPT Algorithm Implementation for Solar Photovoltaic module using microcontroller” India Conference (INDICON), 2011 Annual IEEE pp. 1 - 3
- [2] Lixin Pang, Hui Wang, Yuxia Li, Jian Wang, Ziyu Wang “Analysis of Photovoltaic Charging System Based on MPPT” IEEE. Volume: 2 pp. 498 - 501
- [3] Chih-Chiang Hua, Pi-Kuang Ku “Implementation of a Stand-Alone Photovoltaic Lighting System with MPPT, Battery Charger and High Brightness LEDs”, In proceeding of: Power Electronics and Drive

- Systems, 2003. PEDS 2003, The Fifth International Conference on, Volume: 2
- [4] Xiaolei WANG, Pan Y AN, Liang YANG “An Engineering Design Model of Multi-cell Series-parallel Photovoltaic Array and MPPT Control” Modelling, IEEE Identification and Control (ICMIC), The 2010 International Conference pp. 140 - 144
- [5] F.S.Dos Reis, J.Sebastain "characterization of Conducted Noise Generation for sepic, cuk and Boost Converters Working as Power Factor pre-regulators.", Industrial Electronics, Control, and Instrumentation, 1993, Proceedings of the IECON '93. International Conference pp.965 – 970, vol 2
- [6] M. Calais and V. G. Agelidis, —Multilevel converters for single-phase grid connected photovoltaic systems—an overview in Proc. IEEE Int. Symp.Ind. Electron, 1998, vol. 1, pp. 224–229.
- [7] S. B. Kjaer, J. K. Pedersen, and F. Blaabjerg, —A review of single-phase grid connected inverters for photovoltaic modules. Industry Applications, IEEE Transactions Volume: 41, Issue 5, pp. 1292 - 1306
- [8] E. Villanueva, P. Correa, J. Rodriguez, and M. Pacas, “Control of a single phase cascaded H-bridge multilevel inverter for grid-connected photovoltaic systems,” IEEE Industrial Electronics, IEEE Transactions on Volume: 56 Issue 11, pp. 4399 - 4406
- [9] C. Cecati, F. Ciancetta, and P. Siano, —A multilevel inverter for photovoltaic systems with fuzzy logic control. Journal: IEEE Transactions on Industrial Electronics - IEEE Trans Ind Electron , vol. 57, no. 12, pp. 4115-4125, 2010